Atmospheric Research 295 (2023) 106995

Contents lists available at ScienceDirect

Atmospheric Research

journal homepage: www.elsevier.com/locate/atmosres

Characterisation of vehicle emissions in a road tunnel in Lisbon

I. Cunha-Lopes [a,*], C.A. Alves [b], I. Casotti Rienda [b], F. Lucarelli [c], E. Diapouli [d], S.M. Almeida [a]

[a] Centro de Ciências e Tecnologias Nucleares, Instituto Superior Técnico, Universidade de Lisboa, Estrada Nacional 10, 2695-066 Bobadela-LRS, Portugal
[b] Centre for Environmental and Marine Studies, Department of Environment, University of Aveiro, 3810-193 Aveiro, Portugal
[c] INFN - Firenze, National Institute for Nuclear Physics - Florence division, Sesto Fiorentino, Italy
[d] Institute of Nuclear & Radiological Sciences and Technology, Energy & Safety, National Centre for Scientific Research "Demokritos", Agia Paraskevi, Athens, 15310, Greece

ARTICLE INFO

Keywords:
Vehicle pollutants
Real-world measurements
Particulate matter
OC/EC
Emission factors

ABSTRACT

In urban areas, road traffic is one of the main sources of air pollutants, mainly as particulate matter (PM). Knowledge about fingerprints of vehicle emissions under real-world driving conditions is scarce for Europe, especially in Portugal. The aim of this study was to characterise and quantify vehicle emissions through road tunnel measurements. The sampling campaign was carried out during one week inside a road tunnel and simultaneously in an urban background site in Lisbon. $PM_{2.5}$ and $PM_{2.5–10}$ filters were analysed by PIXE for elemental composition and by a thermal-optical transmittance technique for the determination of organic carbon (OC) and elemental carbon (EC). $PM_{2.5}$ and PM_{10} concentrations were, at least, 20 and 10 times higher than those found in the background, respectively. Inside the tunnel, particle organic matter (POM), EC and other anthropogenic compounds accounted for more than 90.0% of the $PM_{2.5}$ mass. Fe, Ca, Si, S and Cu represented 88.7% of the $PM_{2.5}$-bound elements, while Fe, Cl, Ca, Si, Cu, Zn, Na, S, Ba mostly contributed to the $PM_{2.5–10}$ elemental mass fraction (93.8%). Total carbon represented about 58.5% of $PM_{2.5}$ and 26.5% of $PM_{2.5–10}$. EC presented a high tunnel/background ratio (T/B = 35.4 for $PM_{2.5}$ and 48.8 for $PM_{2.5–10}$). Cu, Fe, Cr, Ba, Mn, Zn and Rb, which are key tracers of tyre and brake wear, showed a T/B > 70 and very good correlations between them. The emission factors (*EF*) of $PM_{2.5}$ and PM_{10} were estimated to be 139 ± 20.7 and 172 ± 23.9 mg veh^{-1} km^{-1}. The average *EF* of OC and EC in $PM_{2.5}$ were 30.9 ± 6.48 and 44.6 ± 7.33 mg veh^{-1} km^{-1}. This real-world study contributes to define road traffic emission profiles in urban areas, provide data to update European emission inventories, and evaluate the impact of traffic-generated PM on human health and the environment.

1. Introduction

Air pollution is the single largest environmental health risk in Europe. The vast majority of the urban population is exposed to unsafe levels that can lead to harmful effects on human health and the environment (EEA, 2021). In urban areas, road traffic is one of the main sources of air pollutants, mainly from particulate matter (PM) (Amato et al., 2016; Byčenkiene et al., 2014; Custódio et al., 2016). Black carbon (BC) from the incomplete combustion of carbonaceous fuels is one of the main constituents of $PM_{2.5}$ (Moreno et al., 2015). It is considered a unique primary tracer for combustion as it has no other sources (Bachmann, 2009; Moreno et al., 2015). It also affects the optical properties of the atmosphere and it is recognised as one of the most important anthropogenic forcing agent for climate change. (EPA, 2023) Road transport is a source of exhaust emissions resulting from combustion and non-exhaust emissions. The latter include particles from brake and tyre wear, road surface abrasion and dust resuspension (Alves et al., 2018; Casotti Rienda and Alves, 2021; Thorpe and Harrison, 2008). Data from European cities showed that exhaust and non-exhaust sources contribute equal amounts to total traffic-related emissions (Amato et al., 2014; EEA, 2020). However, strict policies only have led to sizeable reductions in exhaust emissions (Casotti Rienda and Alves, 2021; Gasser et al., 2009; Gualtieri et al., 2008), while the toxicity of non-exhaust emissions is not well documented (OECD, 2020; Schwarze et al., 2013). Several technologies have been introduced to vehicles to achieve lower emissions and meet the increasingly stringent emission standards. Nevertheless, knowledge about the fingerprints of vehicle sources in real-world driving and the contribution of exhaust and non-exhaust emissions to airborne particulate matter levels is scarce in Europe, especially in Portugal (Alves et al., 2015; Handler et al., 2008; Pio et al., 2013).

* Corresponding author.
E-mail address: ines.lopes@ctn.tecnico.ulisboa.pt (I. Cunha-Lopes).

https://doi.org/10.1016/j.atmosres.2023.106995
Received 28 June 2023; Received in revised form 1 September 2023; Accepted 1 September 2023
Available online 4 September 2023

Diverse approaches have been used to measure vehicle emissions. These measurements can be studied under controlled laboratory conditions (e.g., chassis dynamometer methods) or under realistic driving conditions, such as in tunnels. These underground infrastructures provide excellent experimental conditions because traffic-related pollutants are confined inside, thus minimising dilution with ambient air. Moreover, tunnel studies also reflect the real traffic driving conditions, representing the mix of exhaust and non-exhaust emissions (Alves et al., 2016; Brimblecombe et al., 2015; Handler et al., 2008; McGaughey et al., 2004; Pio et al., 2013).

Through road tunnel measurements, the objective of this paper was to obtain PM emission factors and chemical profiles of road traffic emissions. This study will contribute to update European emission inventories, and to the new database of atmospheric particulate matter emission source profiles in Europe (SPECIEUROPE), thus improving the source apportionment capabilities of receptor models.

2. Materials and Methods

2.1. Road tunnel measurements

2.1.1. Sampling site and design

A sampling campaign was carried out between 21st and 29th October 2019 in Lisbon, the westernmost capital in mainland Europe. Lisbon is the largest city of Portugal with a population density of 5457 inhabitants km^{-2} in 2021. The dominant source of air pollutants is road traffic (Almeida et al., 2009).

The measurement campaign was conducted simultaneously at two sampling points (Fig. 1), one in an urban background site not exposed to direct emissions from traffic and the other one inside the João XXI road tunnel. This two-way tunnel establishes the connection between Campo Pequeno (next to Defensores de Chaves Avenue) and Afonso Costa Avenue in Areeiro, which are two important centralities of Lisbon. It has

Fig. 1. Geographic location of the sampling sites in Lisbon (Portugal). Yellow line indicates the length of the road tunnel; Blue dot indicates the sampling point inside the tunnel; Red dot indicates the background sampling site. (For interpretation of the references to colour in this figure legend, the reader is referred to the web version of this article.)

a length of 1768 m and permits traffic in both directions, having two lanes on each side and two secondary exits, one to Almirante Reis Avenue and the second next to Gago Coutinho Avenue. It possesses a cross ventilation system to extract pollutants that is turned on during rush hours, when CO reaches critical levels. This tunnel is located within Zone 2 of the Low Emission Zone (LEZ), which specifically means that light-duty vehicles (LDV) manufactured before January 1996 and heavy-duty vehicles (HDV) before October 1996 cannot be driven within this zone.

Traffic volume by vehicle type through the tunnel was manually counted in one way (closest to the equipment) during the sampling periods on weekdays. Traffic count data was grouped as LDV, HDV and motorcycles (MCV). LDV comprise passenger cars and light commercial vehicles, while HDV encompass heavy trucks weighing less than 10 tons, as vehicles exceeding 10 tons are prohibited inside the tunnel. There was no record of bus circulation inside the tunnel. It was not possible to distinguish between diesel and petrol vehicles, so for calculations, the vehicle fleet for Portugal in 2019 was considered (APA, 2022).

2.1.2. Pollutant sampling and measurement

The pollutants measured in each sampling site were $PM_{2.5}$ (fine fraction), $PM_{2.5–10}$ (coarse fraction), and NOx.

- **PM** samplers MVS6 Leckel (Sven Leckel, Germany) were used to collect simultaneously $PM_{2.5}$ and $PM_{2.5–10}$ (by a sampling head developed by the Institute of Nuclear and Radiological Sciences and Technology, Energy and Safety, N.C.S.R. Demokritos) at a constant flow rate of 2.3 m^3 h^{-1}. One sampler collected $PM_{2.5}$ onto polytetrafluoroethylene filters (PTFE; Whatman; 47 mm in diameter, 2.0 μm pore size) and $PM_{2.5–10}$ onto Nucleopore filters (Whatman; 25 mm in diameter, 0.4 μm pore size). The other sampler collected $PM_{2.5}$ and $PM_{2.5–10}$ onto quartz filters (Pall, LifeSciences) with 47 mm and 25 mm in diameter, respectively. Inside the tunnel, the instruments were properly installed on the roadside. PM sampling was performed in four daily periods of two hours each (8:00–10:00, 10:30–12:30, 14:30–16:30 and 17:00–19:00). With the aim of evaluating the ambient concentrations, which were deemed to be lower, the sampler installed in the background collected PM during a twelve-hour period (8:00–20:00).
- **NOx** was recorded by chemiluminescence real time analysers with 1-min time resolution. Inside the road tunnel a NOx Analyser (Model 42C, Thermo Electron Corporation) was used. Outdoor data was obtained from the Olivais urban background air quality station located close to the background site.

2.2. Analytical determinations

2.2.1. PM mass concentrations

PTFE and polycarbonate filters used in the PM samplers were weighed before and after sampling by means of a microbalance following the procedure described in EN12341. After collection and weighting, the filters were stored in a freezer at −20 °C until the chemical analysis.

2.2.2. Elemental composition

PTFE and polycarbonate filters were analysed by particle induced X-ray emission (PIXE), as described by Lucarelli et al. (2018), to measure the concentrations of elements with atomic number Z > 10 (Na, Mg, Al, Si, P, S, Cl, K, Ca; Ti, V, Cr, Mn, Fe, Ni, Cu, Zn, As, Se, Br, Rb, Sr, Y, Zr, Mo, Ba, Pb). PIXE measurements of elements starting from Na were done at LABEC (University of Florence) using a 3 MeV proton beam. Data analysis was performed using the GUPIXWIN software.

2.2.3. Carbonaceous content

PM quartz filters were analysed by a thermal-optical transmittance technique for the determination of organic carbon (OC) and elemental carbon (EC).

In the fine fraction, OC was vaporised in a nitrogen atmosphere up to 600 °C. Then, EC was determined by sequential heating to 850 °C in an atmosphere containing 4% oxygen. The carbon released in the various steps, in the form of CO_2, was quantified by a non-dispersive infrared (NDIR) analyser. Monitoring of the light transmittance through the filter with a laser beam allowed for correcting the EC formed by pyrolysis of the OC during the first heating step from the one that was originally present in the filter (Pio et al., 2011).

The coarse fraction was analysed in an OC-EC Aerosol Analyser from Sunset Laboratory Inc. For the determination of OC and EC on a routine basis, the EUSAAR-2 thermal protocol was used (Karanasiou et al., 2011).

2.3. Mass closure

Mass closure was performed to determine the contribution of possible emission sources to the total PM_{10} mass. Elements were grouped into three main emission sources (Table 1): Mineral dust, Sea Salt and Anthropogenic based on a priori knowledge of inorganic markers associated with the emission sources (Calvo et al., 2013). Furthermore, the EC and particle organic matter (POM) sources were also taken into account. The sum of the chemical species in the aerosol with values lower than the total mass concentration corresponds to the unidentified mass (UM) that represents unanalysed constituents, as well as unaccounted particle-bound water.

POM was calculated by multiplying OC by a factor of 1.6 to consider the atoms (e.g., H, N, O) that are associated with the organic mass (Polidori et al., 2008) and that cannot be measured by thermal-optical analytical techniques. Mineral dust was calculated using the typical crustal ratios with respect to aluminum (Wedepohl, 1995): Mg/Al = 0.170, K/Al = 0.370, Ca/Al = 0.380, Fe/Al = 0.400 and Ba/Al = 0.0100. For sea salt, major sea salt components and typical elemental ratios for sea water, such as Mg/Na = 0.119, K/Na = 0.0370, Ca/Na = 0.0380 and SO_4^{2-}/Na = 0.253, were assumed (Almeida et al., 2006; Calzolai et al., 2015). For anthropogenic sources, elements that have an origin other than anthropogenic were estimated by [anthrop.X] = [TotalX] - [soilX] - [seasaltX], where X is the element.

It should be noted that the presence of common oxides was assumed in mineral dust and anthropogenic source, so element concentrations were multiplied by a stoichiometric factor to account for the oxygen mass. Moreover, all elements were considered, including values below the detection limit, which were substituted by half of its value.

2.4. Emission factors

EF are functional relations defined as “the mass (or number) of pollutant released per unit time/distance travelled or mass of fuel used” and typically depend on conditions at the sampling site, traffic intensity and modal shares of HDVs and LDVs (Imhof et al., 2005; Staehelin et al., 1995). In this study, the daily *EF* (mg km^{-1} veh^{-1}) for $PM_{2.5}$, PM_{10}, carbonaceous components and chemical elements were calculated as follows (Pant and Harrison, 2013).

$$EF_p = \Delta C_p \times D / N_{tot\ al} \quad (1)$$

Table 1
Compounds associated with emission sources.

POM	1.6 × [OC]
Mineral Dust	1.89 × [Al] + 2.14 × [Si] + [Ti] + [P] + [Mn] + [soilMg] + [soilK] + 1.4 × [soilCa] + 1.43 × [soilFe] + [soilBa] + [Sr]
Sea Salt	[Na] + [Cl] + [Mg] + [ssK] + [ssCa] + [$ssSO_4^{2-}$]
Anthropogenic elements	[anthrop.K] + 1.4 × [anthrop.Ca] + 1.43 × [anthrop.Fe] + [V] + [Cr] + [Ni] + [Cu] + [Zn] + [As] + [Se] + [Br] + [Rb] + [Sr] + [Y] + [Zr] + [Mo] + [anthrop.Ba] + [Pb] + 2.99 × [anthrop.SO_4^{2-}]

Table 2
PM mass fractions (average wt ± SD %) and concentrations (mass concentration ± SD ng m^{-3}) of chemical constituents.

		$PM_{2.5}$ ± SD		$PM_{2.5–10}$ ± SD	
		Tunnel	Background	Tunnel	Background
OC	wt%	26.0 ± 7.75	39.4 ± 12.5	16.4 ± 7.29	12.4 ± 6.82
	ng m^{-3}	30,100 ± 7760	3960 ± 1360	5400 ± 1680	1000 ± 211
EC	wt%	32.4 ± 7.64	10.5 ± 4.07	10.2 ± 6.30	0.688 ± 0.568
	ng m^{-3}	38,560 ± 11,400	1100 ± 471	3160 ± 837	66.9 ± 58.0
Na	wt%	0.159 ± 0.138	1.89 ± 1.45	0.583 ± 0.422	1.92 ± 0.532
	ng m^{-3}	171 ± 117	176 ± 99.5	227 ± 200	183 ± 75.9
Mg	wt%	0.119 ± 0.0479	0.332 ± 0.212	0.209 ± 0.0721	0.385 ± 0.0787
	ng m^{-3}	141 ± 58.8	31.5 ± 16.1	76.3 ± 37.9	37.0 ± 12.7
Al	wt%	0.297 ± 0.0678	0.482 ± 0.169	0.339 ± 0.167	0.413 ± 0.184
	ng m^{-3}	356 ± 111	48.5 ± 19.8	111 ± 29.0	41.4 ± 26.0
Si	wt%	0.975 ± 0.282	1.35 ± 0.347	1.01 ± 0.440	1.12 ± 0.432
	ng m^{-3}	1180 ± 434	135 ± 46.1	334 ± 88.3	113 ± 66.4
P	wt%	0.0573 ± 0.0132	0.0769 ± 0.0766	0.0389 ± 0.0326	0.0465 ± 0.0277
	ng m^{-3}	68.7 ± 22.1	6.22 ± 4.02	11.7 ± 4.90	3.97 ± 1.94
S	wt%	0.780 ± 0.446	3.77 ± 1.75	0.559 ± 0.252	0.663 ± 0.0729
	ng m^{-3}	886 ± 443	407 ± 265	188 ± 70.8	66.8 ± 25.4
Cl	wt%	0.354 ± 0.253	1.28 ± 1.44	2.34 ± 2.00	5.36 ± 2.37
	ng m^{-3}	393 ± 236	105 ± 90.5	923 ± 880	532 ± 321
K	wt%	0.180 ± 0.0907	1.19 ± 0.846	0.161 ± 0.0741	0.393 ± 0.102
	ng m^{-3}	211 ± 106	144 ± 144	59.0 ± 37.6	36.8 ± 9.00
Ca	wt%	1.68 ± 0.646	1.97 ± 1.13	2.07 ± 0.748	2.57 ± 1.25
	ng m^{-3}	2050 ± 910	182 ± 82.8	715 ± 282	225 ± 80.4
Ti	wt%	0.0773 ± 0.0196	0.0676 ± 0.0261	0.0921 ± 0.0515	0.0536 ± 0.0127
	ng m^{-3}	92.4 ± 29.3	6.42 ± 2.07	29.1 ± 5.06	5.33 ± 2.16
V	wt%	0.0172 ± 0.00930	0.0378 ± 0.0171	0.0168 ± 0.00761	0.00468 ± 0.00285
	ng m^{-3}	19.9 ± 10.4	4.01 ± 2.50	5.56 ± 2.19	0.500 ± 0.407
Cr	wt%	0.0853 ± 0.0223	0.0165 ± 0.00434	0.156 ± 0.0977	0.0148 ± 0.00566
	ng m^{-3}	103 ± 34.7	1.59 ± 0.271	48.8 ± 9.02	1.38 ± 0.566
Mn	wt%	0.0958 ± 0.0235	0.0212 ± 0.00905	0.189 ± 0.102	0.0240 ± 0.00968
	ng m^{-3}	115 ± 37.0	2.04 ± 0.910	60.2 ± 10.0	2.25 ± 0.952
Fe	wt%	12.1 ± 2.36	1.88 ± 0.783	21.7 ± 12.1	2.12 ± 0.715
	ng m^{-3}	14,500 ± 4030	187 ± 82.2	6874 ± 1100	206 ± 92.2
Ni	wt%	0.00853 ± 0.00233	0.0152 ± 0.00576	0.00828 ± 0.00371	0.00263 ± 0.00225
	ng m^{-3}	10.2 ± 3.36	1.63 ± 1.08	2.78 ± 1.26	0.303 ± 0.332
Cu	wt%	0.450 ± 0.0982	0.0588 ± 0.0243	0.701 ± 0.404	0.0653 ± 0.0343
	ng m^{-3}	539 ± 162	5.79 ± 2.40	222 ± 43.9	6.19 ± 3.52
Zn	wt%	0.199 ± 0.0420	0.0920 ± 0.0269	0.741 ± 1.56	0.455 ± 0.500
	ng m^{-3}	239 ± 71.5	9.56 ± 3.73	168 ± 154	43.9 ± 51.0
As	wt%	0.00273 ± 0.00154	0.00988 ± 0.00251	0.00244 ± 0.00178	0.000885 ± 0.000582
	ng m^{-3}	3.30 ± 1.88	1.04 ± 0.453	0.766 ± 0.273	0.0753 ± 0.0322
Se	wt%	0.00303 ± 0.00115	0.00542 ± 0.00336	0.00245 ± 0.00130	0.000706 ± 0.000235
	ng m^{-3}	3.52 ± 1.29	0.602 ± 0.556	0.808 ± 0.257	0.0693 ± 0.0354
Br	wt%	0.00644 ± 0.00344	0.0280 ± 0.00652	0.00367 ± 0.00318	0.00375 ± 0.00208
	ng m^{-3}	7.24 ± 3.52	3.03 ± 1.49	1.09 ± 0.362	0.341 ± 0.202
Rb	wt%	0.0344 ± 0.0132	0.00811 ± 0.00423	0.111 ± 0.0475	0.00203 ± 0.000843
	ng m^{-3}	42.2 ± 20.4	0.803 ± 0.356	39.1 ± 18.9	0.204 ± 0.119
Sr	wt%	0.00952 ± 0.00122	0.0110 ± 0.00521	0.0165 ± 0.00476	0.00329 ± 0.00153
	ng m^{-3}	11.1 ± 1.95	1.04 ± 0.270	5.86 ± 2.00	0.309 ± 0.157
Y	wt%	0.0102 ± 0.00285	0.0146 ± 0.00741	0.0181 ± 0.0190	0.00270 ± 0.00119
	ng m^{-3}	11.8 ± 3.22	1.34 ± 0.381	5.24 ± 1.67	0.263 ± 0.138
Zr	wt%	0.0475 ± 0.01621	0.0242 ± 0.0148	0.0574 ± 0.0221	0.00363 ± 0.00108
	ng m^{-3}	57.5 ± 24.0	2.11 ± 1.04	19.9 ± 8.43	0.342 ± 0.144
Mo	wt%	0.0214 ± 0.00980	0.0416 ± 0.0188	0.0204 ± 0.0116	0.00775 ± 0.0127
	ng m^{-3}	25.4 ± 11.2	3.76 ± 0.655	6.64 ± 3.15	0.748 ± 1.26
Ba	wt%	0.2536 ± 0.0657	0.0494 0.0306	0.481 ± 0.276	0.0473 ± 0.0181
	ng m^{-3}	305 ± 103	4.50 ± 1.96	152 ± 24.2	4.42 ± 1.83
Pb	wt%	0.00718 ± 0.00290	0.00906 ± 0.00265	0.00546 ± 0.00359	0.00245 ± 0.00256
	ng m^{-3}	8.27 ± 2.97	0.868 ± 0.129	1.72 ± 0.452	0.193 ± 0.148
TC	wt%	58.5 ± 8.34	49.9 ± 17.2	26.5 ± 7.47	13.1 ± 7.59
	ng m^{-3}	71,100 ± 3410	5060 ± 1431	9660 ± 1439	1050 ± 456
∑ elements	wt%	18.1 ± 3.30	14.7 ± 3.45	31.6 ± 16.1	15.7 ± 2.98
	ng m^{-3}	24,700 ± 3150	1600 ± 117	11,300 ± 1447	1560 ± 113

where ΔC_p (mg m^{-3}) is the difference in concentration of pollutant p between the tunnel and background, and N_{total} is the total number of vehicles crossing the sampling point per measuring period. It is assumed that both NOx and PM have similar dilution. D is the dilution rate, which is calculated by:

$$\boldsymbol{D} = \boldsymbol{N_{LDV}} \times \boldsymbol{EF_{NO_{xLDV}}} + \boldsymbol{N_{HDV}} \times \boldsymbol{EF_{NO_{xHDV}}} + \boldsymbol{N_{MCV}} \times \boldsymbol{EF_{NO_{xMCV}}} / \boldsymbol{\Delta C_{NO_x}} \quad (2)$$

where, N is the number of vehicles (per measuring period) and EF_{NOx} is the emission factor for NOx (in mg km^{-1}) for each vehicle category. ΔC_{NOx} is the difference in NOx concentration between the tunnel and background (mg m^{-3}). To consider the different fuel types and EURO categories, the weighted average of EF_{NOx} values for LDV, HDV and MCV were calculated taking into account the vehicle fleet for Portugal in 2019 (APA, 2022).

3. Results and discussion

3.1. Traffic density and pollutant concentrations

Traffic passing through the tunnel was dominated by LDV (94.6%), followed by MCV (4.55%) and HDV (0.83%). Traffic density varied between 1960 and 2590 vehicles per measuring period (2 h) in one way. During rush hours (8:00–10:00 h and 17:00–19:00 h), the number of vehicles passing through the tunnel increased (on average, 2560 vehicles per measuring period) compared to the other measuring periods (10:30–12:30 and 14:30–16:30, 2110 vehicles per measuring period).

Inside the tunnel, the mean $PM_{2.5}$ and PM_{10} concentration was 129 ± 12.4 μg m^{-3} and 168 ± 17.2 μg m^{-3}, respectively. The Wilcoxon Matched pairs test was applied. Statistically significant differences were observed between the $PM_{2.5}$ ($p < 0.0018$) and PM_{10} ($p < 0.0077$) inside the tunnel and in the background location. In the background atmosphere, these concentrations were, at least, 20 and 10 times lower, respectively. The lowest PM concentration mean value was measured on Sunday ($PM_{2.5}$ = 106 μg m^{-3}, PM_{10} = 136 μg m^{-3}), as normally there is no rush hour, and the traffic flow is less than during weekdays. On average, inside the tunnel, $PM_{2.5}$ represented 76.8% of PM_{10}, while a share of 52.0% was recorded in the background air. These results reflect the high contribution of traffic for the emission of fine particles. Previous road tunnel studies have already shown high pollutant concentrations inside tunnels since there is little dilution of traffic emissions (Alves et al., 2015; Brimblecombe et al., 2015; Marinello et al., 2020).

3.2. Chemical characterisation

3.2.1. Elements and carbonaceous constituents

EC, OC and elemental $PM_{2.5}$ and $PM_{2.5–10}$ mass fractions and concentrations are shown in Table 2. Inside the tunnel, the sum of elements accounted for 18.1 ± 3.30 and 31.6 ± 16.1% of $PM_{2.5}$ and $PM_{2.5–10}$, respectively, while in the background location the mass fractions were 14.7 ± 3.45 and 15.7 ± 2.98% for $PM_{2.5}$ and $PM_{2.5–10}$, respectively.

Inside the tunnel, Fe was the most abundant element, accounting for 12.1 ± 2.36% in $PM_{2.5}$ and 21.7 ± 12.1% in $PM_{2.5–10}$. The ratio between the tunnel and the background for the fine fraction stood out (T/B = 101; Fig. S1) for this element, as well for Cu, Cr, Ba, Mn and Rb (T/B > 70). These elements had a very good correlation (Fe vs Cr, Fe vs Mn, Fe vs Cu, Fe vs Ba– $r^2 \geq 0.900$ and Fe vs Rb – $r^2 = 0.671$) between them (Fig. 2), indicating a common source. Previous studies have already shown that these elements are key tracers of tyre and brake wear (Grigoratos and Martini, 2015; Hagino et al., 2016). In a study in another urban road tunnel in Lisbon, Pio et al. (2013) reported that Cu levels were strongly correlated with Fe, Mn, and Cr in all size ranges ($PM_{0.5}$, $PM_{0.5–1}$, $PM_{1–2.5}$, and $PM_{2.5–10}$), suggesting that these metals have a common source across different particle sizes. It should be noted that in the fine fraction, T/B of Zn was 28.1, presenting a good correlation with the other elements. In the coarse fraction, the Zn tunnel/background ratio was lower (T/B = 5.20) and the correlation with Fe was $r^2 = 0.793$, after exclusion of some outliers (triangle symbol in Fig. 2), suggesting that there is another source of Zn contributing to its concentration. Inside the tunnel, 5 elements (Fe, Ca, Si, S and Cu) represented 88.7% of the total concentrations of elements determined in $PM_{2.5}$, while the coarse fraction was dominated by 9 elements (Fe, Cl, Ca, Si, Cu, Zn, Na, S, and Ba), which accounted for 93.8% of the overall mass of elements. Typical elements of tyre and brake wear (Grigoratos and Martini, 2015; Sommer et al., 2018), such as Cu, Zn and Ba, were present in high concentrations in the coarse fraction. Cunha-Lopes et al. (2022) chemically characterised the thoracic fraction of road dust (PM_{10}) in Lisbon, reporting Cu and Zn as the most enriched elements in relation to the soil composition. In the urban background, in both size fractions, the predominant elements were Na, Mg, Al, Si, S, Cl, K and Ca. Furthermore, in this site, Fe was also an element that presented a high mass fraction in relation to the remaining composition. Fig. 2 presents the regressions since this information is essential to provide support in identifying the sources. The characterisation of the source profiles and the assessment of the relation between elements are very important for researchers working with receptor models.

Total carbon (TC=OC + EC) accounted for 58.5 ± 8.34% of $PM_{2.5}$ and 26.5 ± 7.47% of $PM_{2.5–10}$ inside the tunnel. As expected, a high tunnel/background ratio was observed for EC (T/B = 35.4 for $PM_{2.5}$ and 48.8 for $PM_{2.5–10}$), since this carbonaceous constituent is associated with exhaust and non-exhaust emissions (Amato et al., 2011; Hao et al., 2019). In this study, the OC and EC mass fractions in $PM_{2.5}$ inside the tunnel were 26.0 ± 7.75% and 32.4 ± 7.64%, respectively, while in the background air were 39.4 ± 12.5% and 10.5 ± 4.07%. For the coarse fraction, in the road tunnel, the mass fractions of OC and EC were 16.4 ± 7.29% and 10.2 ± 6.30%, respectively, whereas in the background they represented 12.4 ± 6.82% and 0.688 ± 0.568%, respectively. Alves et al. (2015) carried out a sampling campaign inside an urban road tunnel in northern Portugal, mainly impacted by LDVs, and obtained similar carbonaceous fractions in $PM_{2.5}$ (OC = 24.4% and EC = 26.9%). In a Shanghai road tunnel, Zhou et al. (2014) registered TC mass fractions in $PM_{2.5}$ from 41.0% to 61.1%, very similar to those of this study. The mean OC/EC ratio in $PM_{2.5}$ was 1.85. Inside tunnels there is less light and more concentration of EC due to the traffic source, so the OC/EC ratio is commonly not higher than 2 (Brito et al., 2013; Handler et al., 2008; Zhou et al., 2014).

3.2.2. Mass closure

The mass concentrations of $PM_{2.5}$ and $PM_{2.5–10}$ were reconstructed by adding the PM chemical components. Elements were grouped into

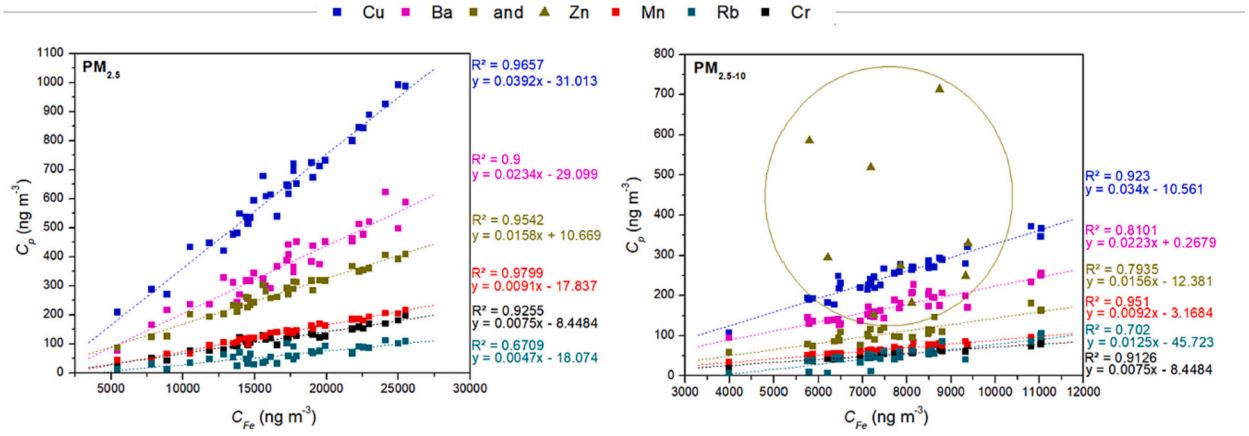

Fig. 2. Correlation between the concentrations of Fe and other elements (Cr, Mn, Cu, Rb, Ba and Zn) in the fine and coarse size fractions.

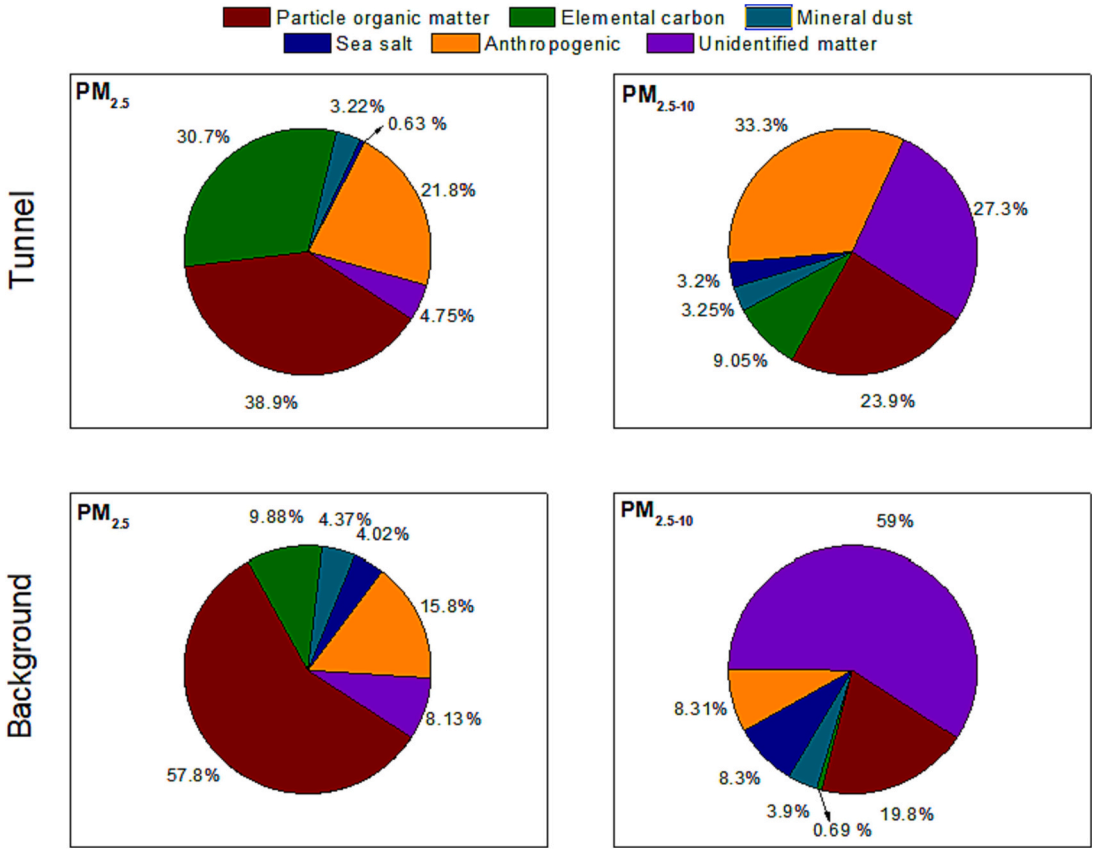

Fig. 3. A – Mass closure of the $PM_{2.5}$ and $PM_{2.5–10}$ mass fractions in the road tunnel and in the urban background atmosphere.

three main sources (mineral dust, sea salt and anthropogenic constituents), to which POM, EC and unanalysed constituents were added, as showed in Fig. 3.

Inside the tunnel, on average, the identified matter accounted for 95.2 and 72.7% of the $PM_{2.5}$ and $PM_{2.5–10}$ mass, respectively. In the background, on average, the analysed chemical compounds accounted for 91.9 and 41.0% of $PM_{2.5}$ and $PM_{2.5–10}$ mass, respectively. For the coarse fraction, a significant portion of the mass concentration was not speciated. This unalysed matter is likely related to unidentified/unquantified elements and particle-bound water. Previous studies have already shown the influence of particle-adsorbed water, which can play a significant role in the physical and chemical properties of PM (Widziewicz-Rzońca and Tytła, 2020).

In this study, POM, EC and anthropogenic elements represented more than 90% of the $PM_{2.5}$ mass inside the tunnel. As shown in subchapter 3.2.1, the carbonaceous material was predominantly concentrated in the fine PM fraction. Particle organic matter (38.9% in the tunnel and 57.8% in the background) was the dominant contributor to the total mass of $PM_{2.5}$ for both sites. The sources of POM are diverse and complex. In the tunnel, POM can be predominantly associated with the OC from both exhaust and non-exhaust emissions from traffic, while in the urban background air, biogenic emissions, other anthropogenic sources (e.g., cooking), and secondarily formed organic aerosols also contribute to the PM levels. Faria et al. (2022) carried out a study in Lisbon and showed that POM was the dominant contributor to the total PM mass outside homes (36%) and schools (42%).

3.3. Emission factors

Road vehicle emissions are influenced by a wide range of parameters and there are different ways to determine *EF*. Previous studies have already calculated *EF* in different conditions as input to emission inventories and to help with the adoption of appropriate air quality plans (Franco et al., 2013). *EF* of $PM_{2.5}$, PM_{10}, carbonaceous constituents and various chemical elements, estimated using Eq. 1, are shown in Table 3. To estimate *EF*, it was necessary to calculate the EF_{NOx} for the different

Table 3
Emission factors determined for $PM_{2.5}$ and PM_{10} in mg veh $^{-1}$ km^{-1}.

	EF $PM_{2.5}$ ± SD	PM_{10} ± SD
	mg veh^{-1} km^{-1}	
PM	139 ± 21	172 ± 23.9
OC	30.9 ± 6.48	35.3 ± 7.15
EC	44.6 ± 7.33	51.0 ± 9.12
Mg	0.173 ± 0.0368	0.208 ± 0.0405
Al	0.466 ± 0.0918	0.558 ± 0.109
Si	1.58 ± 0.339	1.87 ± 0.388
P	0.0806 ± 0.0104	0.0900 ± 0.0122
S	0.537 ± 0.107	0.665 ± 0.126
Cl	0.326 ± 0.136	0.444 ± 0.494
K	0.169 ± 0.0209	0.186 ± 0.0403
Ca	2.83 ± 0.532	3.50 ± 0.652
Ti	0.121 ± 0.0177	0.151 ± 0.0189
V	0.0183 ± 0.00254	0.0250 ± 0.00348
Cr	0.148 ± 0.0270	0.205 ± 0.0304
Mn	0.165 ± 0.0281	0.236 ± 0.0331
Fe	20.2 ± 3.52	28.3 ± 4.13
Ni	0.0116 ± 0.00204	0.0145 ± 0.00217
Cu	0.773 ± 0.137	1.04 ± 0.156
Zn	0.331 ± 0.0591	0.506 ± 0.1491
As	0.00286 ± 0.00116	0.00387 ± 0.00120
Se	0.00306 ± 0.000725	0.00400 ± 0.000789
Br	0.00459 ± 0.00171	0.00565 ± 0.00153
Rb	0.0733 ± 0.0111	0.129 ± 0.0221
Sr	0.0126 ± 0.00235	0.0200 ± 0.00314
Y	0.0136 ± 0.00695	0.0200 ± 0.00694
Zr	0.0747 ± 0.0106	0.102 ± 0.0185
Mo	0.0331 ± 0.0151	0.0700 ± 0.0515
Ba	0.442 ± 0.0747	0.625 ± 0.0888
Pb	0.00882 ± 0.00245	0.0107 ± 0.00269

Table 4
Comparison between *EF* determined for PM_{10} (mg veh^{-1} km^{-1}) in this study and in previous road tunnel studies.

	João XXI tunnel, Lisbon (this study)	Kamshet-I tunnel, India (Raparthi and Phuleria, 2022)	Liberdade Avenue tunnel, Braga, PT (Alves et al., 2015)	Kaisermühlen tunnel, Vienna, AT (Handler et al., 2008)
Cu	1.04 ± 0.156	0.106 ± 0.024	0.11	0.16
Ba	0.625 ± 0.0888	0.123 ± 0.037	0.67	0.06
Zn	0.506 ± 0.1491	0.694 ± 0.36	0.19	0.16
Cr	0.205 ± 0.0304	0.842 ± 1.603	0.06	

vehicle types, as previously mentioned in sub-chapter 2.4. The weighted mean EF_{NOx} obtained was 655 mg km^{-1} veh^{-1} for LDV, 126 mg km^{-1} veh^{-1} for MCV and for 1740 mg km^{-1} veh^{-1} for HDV. Although LDV and MCV represented a higher percentage of vehicles that circulated in the tunnel, EF_{NOx} for HDV presented a higher value and cannot be ignored.

On average *EF* of $PM_{2.5}$ and PM_{10} were 139 ± 20.7 and 172 ± 23.9 mg veh^{-1} km^{-1}, respectively. For $PM_{2.5}$, OC and EC emission factors were 30.9 ± 6.48 and 44.6 ± 7.33 mg veh^{-1} km^{-1}, respectively. For PM_{10}, OC and EC emission factors were 35.3 ± 7.15 and 51.0 ± 9.12 mg veh^{-1} km^{-1}. Alves et al. (2015) carried out a sampling campaign in an urban roadway tunnel in Braga (Portugal) and registered similar values. The OC and EC *EF* were 39 mg veh^{-1} km^{-1} for PM_{10}, while for $PM_{2.5}$ it was 34 and 38 mg veh^{-1} km^{-1}, respectively. For the same tunnel, the PM_{10} and $PM_{2.5}$ *EF* were 152 and 133 mg veh^{-1} km^{-1}, respectively. In the present study, the *EF* of $PM_{2.5}$-bound elements that stood out most were 20.2 ± 3.52, 2.83 ± 0.532 and 1.58 ± 0.339 mg veh^{-1} km^{-1}, for Fe, Ca and Si, respectively. Similar results for most elements were obtained in previous road tunnel studies (Alves et al., 2015; Handler et al., 2008; Raparthi and Phuleria, 2022). The exception was Fe, which exceeded the values previously documented. As shown earlier, in this study Fe presented a high concentration in both size fractions. An earlier study carried out in Lisbon that analysed non-exhaust emissions also reported high concentrations of Fe (Cunha-Lopes et al., 2022). It is known that in urban areas Fe can be enriched in relation to the soil due to the contribution of vehicle brake discs (Querol et al., 2019). The characteristic elements of vehicle emissions that exhibited higher mean *EF* were Cu, Ba, Zn and Cr (1.04 ± 0.156, 0.625 ± 0.0888, 0.506 ± 0.1491, 0.205 ± 0.0304 mg veh^{-1} km^{-1} in PM_{10}, respectively). Table 4 shows that, apart from the varying fleet mixtures in different countries and years, the *EF* of these elements were similar to those of previous studies, except for Cu, whose value was slightly higher. This element displayed an extremely high pollution index in road dust (PM_{10}) resuspension samples collected on different roads in Lisbon (Cunha-Lopes et al., 2022).

4. Conclusions

Road vehicle emissions have a huge contribution to pollutant concentrations in urban areas and depend on many factors, such as technology, age and maintenance of the vehicle, driver's behaviours and characteristics of the pavement. Therefore, real-world on-road measurements performed in tunnels are important because they reflect the actual vehicle emissions. Tunnel studies describe the behaviour of real-world emissions from on-road vehicles given that the traffic source is isolated. This study provided PM profiles for the vehicle fleet in Lisbon, which can also be considered representative of other European countries. The results showed that $PM_{2.5}$ and PM_{10} concentrations were, at least, 20 and 10 times higher than those found in the background atmosphere, respectively. Fe, Ca, Si, S and Cu represented 88.7% of the $PM_{2.5}$ elemental mass fraction inside the tunnel, while, in the coarse fraction, Fe, Cl, Ca, Si, Cu, Zn, Na, S, and Ba dominated (93.8%). Inside the road tunnel, total carbon accounted for about 58.5% of $PM_{2.5}$ and 26.5% of $PM_{2.5–10}$. The mass fraction of EC in $PM_{2.5}$ was 3 times higher than in the background air. A high tunnel/background ratio (T/B = 35.4 for $PM_{2.5}$ and 48.8 for $PM_{2.5–10}$) was registered for EC. Key tracers of tyre and brake wear, such as Cu, Fe, Cr, Ba, Zn, Mn and Rb, presented T/B > 70 and very good correlations between them. Inside the tunnel, the EFs of $PM_{2.5}$ and PM_{10} were 139 ± 21 and 172 ± 23.9 mg veh^{-1} km^{-1}. OC and EC in $PM_{2.5}$ presented mean *EF* of 30.9 ± 6.48 and 44.6 ± 7.33 mg veh^{-1} km^{-1}, respectively.

The information generated in this study is essential to better characterise traffic emissions since there are a scarcity of data under real-world driving conditions in Southern European countries. Furthermore, it is potentially useful for updating European emission inventories, determining source profiles, and applying them in source apportionment studies to determine the contribution of vehicle emissions to the atmospheric aerosol. The vehicle fleet is constantly changing, so more updated studies are always needed. In addition, the improvement of the database on traffic emissions allows the promotion of a more comprehensive understanding of air quality challenges in several European cities. By collecting similar data from various regions, it is possible to develop a unified framework that captures the nuanced variations in emissions profiles caused by different traffic patterns, vehicle technologies, and road infrastructures.

CRediT authorship contribution statement

I. Cunha-Lopes: Conceptualization, Methodology, Formal analysis, Investigation, Writing – original draft, Writing – review & editing, Visualization, Funding acquisition. **C.A. Alves:** Conceptualization, Methodology, Resources, Writing – review & editing, Supervision, Project administration, Funding acquisition. **I. Casotti Rienda:** Investigation, Writing – review & editing, Funding acquisition. **F. Lucarelli:** Resources. **E. Diapouli:** Resources. **S.M. Almeida:** Conceptualization, Methodology, Investigation, Resources, Writing – review & editing, Supervision, Project administration, Funding acquisition.

Declaration of Competing Interest

The authors declare that they have no known competing financial interests or personal relationships that could have appeared to influence the work reported in this paper.

Data availability

Data will be made available on request.

Acknowledgements

Inês Lopes and Ismael Casotti Rienda acknowledge their PhD fellowships (SFRH/BD/147074/2019 and SFRH/BD/144550/2019, respectively) from the Portuguese Foundation for Science and Technology (FCT). The sampling campaign and analytical work were supported by the project "SOPRO: Chemical and toxicological SOurce PROfiling of particulate matter in urban air", POCI-01-0145-FEDER-029574, funded by FEDER through COMPETE2020 – Programa Nacional Competitividade e Internacionalização (POCI) and by national funds (OE), through FCT/MCTES. Thanks are also due to RADIATE (H2020. #824096). We are also grateful for the support to CESAM (UIDB/50017/2020 & UIDP/50017/2020) from FCT/MCTES through national funds,

and co-funding by FEDER, within the PT2020 Partnership Agreement and Compete 2020. Authors also gratefully acknowledge the FCT support through the UIDB/04349/2020 project. OC/EC in $PM_{2.5-10}$ fraction was supported by the European Commission under the Horizon 2020 – Research and Innovation Framework Programme, through the ATMO-ACCESS Integrating Activity under grant agreement No 101008004. A special acknowledgment goes to Prof. Teresa Nunes, from the University of Aveiro, for her support during the OC/EC analyses.

Appendix A. Supplementary data

Supplementary data to this article can be found online at https://doi.org/10.1016/j.atmosres.2023.106995.

References

Almeida, S.M., Pio, C.A., Freitas, M.C., Reis, M.A., Trancoso, M.A., 2006. Approaching PM2.5 and PM2.5 - 10 source apportionment by mass balance analysis, principal component analysis and particle size distribution. Sci. Total Environ. 368, 663–674. https://doi.org/10.1016/j.scitotenv.2006.03.031.

Almeida, S.M., Freitas, M.C., Repolho, C., Dionísio, I., Dung, H.M., Pio, C.A., Alves, C., Caseiro, A., Pacheco, A.M.G., 2009. Evaluating children exposure to air pollutants for an epidemiological study. J. Radioanal. Nucl. Chem. 280, 405–409. https://doi.org/10.1007/s10967-009-0535-3.

Alves, C.A., Gomes, J., Nunes, T., Duarte, M., Calvo, A., Custódio, D., Pio, C., Karanasiou, A., Querol, X., 2015. Size-segregated particulate matter and gaseous emissions from motor vehicles in a road tunnel. Atmos. Res. 153, 134–144. https://doi.org/10.1016/j.atmosres.2014.08.002.

Alves, C.A., Oliveira, César, Martins, N., Mirante, F., Caseiro, A., Pio, C., Matos, M., Silva, H.F., Oliveira, Cristina, Camões, F., 2016. Road tunnel, roadside, and urban background measurements of aliphatic compounds in size-segregated particulate matter. Atmos. Res. 168, 139–148. https://doi.org/10.1016/j.atmosres.2015.09.007.

Alves, C.A., Evtyugina, M., Vicente, A.M.P., Vicente, E.D., Nunes, T.V., Silva, P.M.A., Duarte, M.A.C., Pio, C.A., Amato, F., Querol, X., 2018. Chemical profiling of PM10 from urban road dust. Sci. Total Environ. 634, 41–51. https://doi.org/10.1016/j.scitotenv.2018.03.338.

Amato, F., Pandolfi, M., Moreno, T., Furger, M., Pey, J., Alastuey, A., Bukowiecki, N., Prevot, A.S.H., Baltensperger, U., Querol, X., 2011. Sources and variability of inhalable road dust particles in three European cities. Atmos. Environ. 45, 6777–6787. https://doi.org/10.1016/j.atmosenv.2011.06.003.

Amato, F., Cassee, F.R., Denier van der Gon, H.A.C., Gehrig, R., Gustafsson, M., Hafner, W., Harrison, R.M., Jozwicka, M., Kelly, F.J., Moreno, T., Prevot, A.S.H., Schaap, M., Sunyer, J., Querol, X., 2014. Urban air quality: the challenge of traffic non-exhaust emissions. J. Hazard. Mater. 275, 31–36. https://doi.org/10.1016/j.jhazmat.2014.04.053.

Amato, F., Alastuey, A., Karanasiou, A., Lucarelli, F., Nava, S., Calzolai, G., Severi, M., Becagli, S., Gianelle, V.L., Colombi, C., Alves, C., Custódio, D., Nunes, T., Cerqueira, M., Pio, C., Eleftheriadis, K., Diapouli, E., Reche, C., Minguillón, M.C., Manousakas, M.I., Maggos, T., Vratolis, S., Harrison, R.M., Querol, X., 2016. AIRUSE-LIFE+: a harmonized PM speciation and source apportionment in five southern European cities. Atmos. Chem. Phys. 16, 3289–3309. https://doi.org/10.5194/acp-16-3289-2016.

APA, A.P.A., 2022. National Informative Inventory Report 2022 Portugal. Amadora.

Bachmann, J., 2009. Black Carbon: A Science/Policy Primer. Pew Center on Global Climate Change.

Brimblecombe, P., Townsend, T., Lau, C.F., Rakowska, A., Chan, T.L., Močnik, G., Ning, Z., 2015. Through-tunnel estimates of vehicle fleet emission factors. Atmos. Environ. 123, 180–189. https://doi.org/10.1016/j.atmosenv.2015.10.086.

Brito, J., Rizzo, L.V., Herckes, P., Vasconcellos, P.C., Caumo, S.E.S., Fornaro, A., Ynoue, R.Y., Artaxo, P., Andrade, M.F., 2013. Physical–chemical characterisation of the particulate matter inside two road tunnels in the São Paulo Metropolitan Area. Atmos. Chem. Phys. 13, 12199–12213. https://doi.org/10.5194/acp-13-12199-2013.

Byčenkiene, S., Plauškaite, K., Dudoitis, V., Ulevicius, V., 2014. Urban background levels of particle number concentration and sources in Vilnius, Lithuania. Atmos. Res. 143, 279–292. https://doi.org/10.1016/j.atmosres.2014.02.019.

Calvo, A.I., Alves, C.A., Castro, A., Pont, V., Vicente, A.M., Fraile, R., 2013. Research on aerosol sources and chemical composition: past, current and emerging issues. Atmos. Res. 120–121, 1–28. https://doi.org/10.1016/j.atmosres.2012.09.021.

Calzolai, G., Nava, S., Lucarelli, F., Chiari, M., Giannoni, M., Becagli, S., Traversi, R., Marconi, M., Frosini, D., Severi, M., Udisti, R., Di Sarra, A., Pace, G., Meloni, D., Bommarito, C., Monteleone, F., Anello, F., Sferlazzo, D.M., 2015. Characterization of PM10 sources in the Central Mediterranean. Atmos. Chem. Phys. 15, 13939–13955. https://doi.org/10.5194/acp-15-13939-2015.

Casotti Rienda, I., Alves, C.A., 2021. Road dust resuspension: a review. Atmos. Res. 261, 105740 https://doi.org/10.1016/j.atmosres.2021.105740.

Cunha-Lopes, I., Alves, C.A., Casotti Rienda, I., Faria, T., Lucarelli, F., Querol, X., Amato, F., Almeida, S.M., 2022. Characterisation of non-exhaust emissions from road traffic in Lisbon. Atmos. Environ. 286, 119221 https://doi.org/10.1016/j.atmosenv.2022.119221.

Custódio, D., Cerqueira, M., Alves, C., Nunes, T., Pio, C., Esteves, V., Frosini, D., Lucarelli, F., Querol, X., 2016. A one-year record of carbonaceous components and major ions in aerosols from an urban kerbside location in Oporto, Portugal. Sci. Total Environ. 562, 822–833. https://doi.org/10.1016/j.scitotenv.2016.04.012.

EEA, 2020. Air quality in Europe - 2020 report - EEA Report no 9/2020. EEA Report. https://doi.org/10.2800/786656.

EEA, 2021. Air quality in Europe - 2021 report -Report no. 15/2021. https://doi.org/10.2800/549289.

EPA, U.S.E.P.A., 2023. Climate Change Indicators: Climate Forcing [WWW Document]. URL. https://www.epa.gov/climate-indicators/climate-change-indicators-climate-forcing.

Faria, T., Martins, V., Canha, N., Diapouli, E., Manousakas, M., Fetfatzis, P., Gini, M.I., Almeida, S.M., 2022. Assessment of children's exposure to carbonaceous matter and to PM major and trace elements. Sci. Total Environ. 807, 151021 https://doi.org/10.1016/j.scitotenv.2021.151021.

Gasser, M., Riediker, M., Mueller, L., Perrenoud, A., Blank, F., Gehr, P., Rothen-Rutishauser, B., 2009. Toxic effects of brake wear particles on epithelial lung cells in vitro. Part. Fibre Toxicol. 6, 30. https://doi.org/10.1186/1743-8977-6-30.

Grigoratos, T., Martini, G., 2015. Brake wear particle emissions: a review. Environ. Sci. Pollut. Res. 22, 2491–2504. https://doi.org/10.1007/s11356-014-3696-8.

Gualtieri, M., Mantecca, P., Cetta, F., Camatini, M., 2008. Organic compounds in tire particle induce reactive oxygen species and heat-shock proteins in the human alveolar cell line A549. Environ. Int. 34, 437–442. https://doi.org/10.1016/j.envint.2007.09.010.

Hagino, H., Oyama, M., Sasaki, S., 2016. Laboratory testing of airborne brake wear particle emissions using a dynamometer system under urban city driving cycles. Atmos. Environ. https://doi.org/10.1016/j.atmosenv.2016.02.014.

Handler, M., Puls, C., Zbiral, J., Marr, I., Puxbaum, H., Limbeck, A., 2008. Size and composition of particulate emissions from motor vehicles in the Kaisermühlen-Tunnel, Vienna. Atmos. Environ. 42, 2173–2186. https://doi.org/10.1016/j.atmosenv.2007.11.054.

Hao, Y., Gao, C., Deng, S., Yuan, M., Song, W., Lu, Z., Qiu, Z., 2019. Chemical characterisation of PM 2.5 emitted from motor vehicles powered by diesel, gasoline, natural gas and methanol fuel. Sci. Total Environ. 674, 128–139. https://doi.org/10.1016/j.scitotenv.2019.03.410.

Imhof, D., Weingartner, E., Ordo, C., Buchmann, B., Du, C., 2005. Real-world emission factors of fine and ultrafine aerosol particles for different traffic situations in Switzerland. Environ. Sci. Technol. 39, 8341–8350. https://doi.org/10.1021/es048925s.

Karanasiou, A., Diapouli, E., Cavalli, F., Eleftheriadis, K., Viana, M., Alastuey, A., Querol, X., Reche, C., 2011. On the quantification of atmospheric carbonate carbon by thermal/optical analysis protocols. Atmos. Meas. Tech. 4, 2409–2419. https://doi.org/10.5194/amt-4-2409-2011.

Lucarelli, F., Calzolai, G., Chiari, M., Nava, S., Carraresi, L., 2018. Study of atmospheric aerosols by IBA techniques: the LABEC experience. Nucl. Instruments Methods Phys. Res. Sect. B Beam Interact. Mater. Atoms 417, 121–127. https://doi.org/10.1016/j.nimb.2017.07.034.

Marinello, S., Lolli, F., Gamberini, R., 2020. Roadway tunnels: a critical review of air pollutant concentrations and vehicular emissions. Transp. Res. Part D Transp. Environ. 86, 102478 https://doi.org/10.1016/j.trd.2020.102478.

McGaughey, G.R., Desai, N.R., Allen, D.T., Seila, R.L., Lonneman, W.A., Fraser, M.P., Harley, R.A., Pollack, A.K., Ivy, J.M., Price, J.H., 2004. Analysis of motor vehicle emissions in a Houston tunnel during the Texas Air Quality Study 2000. Atmos. Environ. 38, 3363–3372. https://doi.org/10.1016/j.atmosenv.2004.03.006.

Moreno, T., Reche, C., Rivas, I., Cruz Minguillón, M., Martins, V., Vargas, C., Buonanno, G., Parga, J., Pandolfi, M., Brines, M., Ealo, M., Sofia Fonseca, A., Amato, F., Sosa, G., Capdevila, M., de Miguel, E., Querol, X., Gibbons, W., 2015. Urban air quality comparison for bus, tram, subway and pedestrian commutes in Barcelona. Environ. Res. 142, 495–510. https://doi.org/10.1016/j.envres.2015.07.022.

OECD, 2020. Non-exhaust Particulate Emissons from Road Transport: An Ignored Environmental Policy Challenge. Paris.

Pant, P., Harrison, R.M., 2013. Estimation of the contribution of road traffic emissions to particulate matter concentrations from field measurements: a review. Atmos. Environ. 77, 78–97. https://doi.org/10.1016/j.atmosenv.2013.04.028.

Pio, C., Cerqueira, M., Harrison, R.M., Nunes, T., Mirante, F., Alves, C., Oliveira, C., Sanchez de la Campa, A., Artíñano, B., Matos, M., 2011. OC/EC ratio observations in Europe: Re-thinking the approach for apportionment between primary and secondary organic carbon. Atmos. Environ. 45, 6121–6132. https://doi.org/10.1016/j.atmosenv.2011.08.045.

Pio, C., Mirante, F., Oliveira, César, Matos, M., Caseiro, A., Oliveira, Cristina, Querol, X., Alves, C., Martins, N., Cerqueira, M., Camões, F., Silva, H., Plana, F., 2013. Size-segregated chemical composition of aerosol emissions in an urban road tunnel in Portugal. Atmos. Environ. 71, 15–25. https://doi.org/10.1016/j.atmosenv.2013.01.037.

Polidori, A., Turpin, B.J., Rodenburg, L.A., Maimone, F., Davidson, C.I., 2008. Organic pm2.5: Fractionation by polarity, ftir spectroscopy, and om/oc ratio for the Pittsburgh aerosol. Aerosol Sci. Technol. 42, 233–246. https://doi.org/10.1080/02786820801958767.

Querol, X., Pérez, N., Reche, C., Ealo, M., Ripoll, A., Tur, J., Pandolfi, M., Pey, J., Salvador, P., Moreno, T., Alastuey, A., 2019. African dust and air quality over Spain: is it only dust that matters? Sci. Total Environ. 686, 737–752. https://doi.org/10.1016/j.scitotenv.2019.05.349.

Raparthi, N., Phuleria, H.C., 2022. On-road vehicular emission characterization from the road-tunnel measurements in India: Morphology, emission factors, and sources. Environ. Res. 215, 114295 https://doi.org/10.1016/j.envres.2022.114295.

Schwarze, P.E., Totlandsdal, A.I., Låg, M., Refsnes, M., Holme, J.A., Øvrevik, J., 2013. Inflammation-related effects of diesel engine exhaust particles: Studies on lung cells in vitro. Biomed. Res. Int. 2013 https://doi.org/10.1155/2013/685142.

Sommer, F., Dietze, V., Baum, A., Sauer, J., Gilge, S., Maschowski, C., Gieré, R., 2018. Tire abrasion as a major source of microplastics in the environment. Aerosol Air Qual. Res. 18, 2014–2028. https://doi.org/10.4209/aaqr.2018.03.0099.

Staehelin, J., Schpferb, K., Biirgin, T., Steinemannd, U., Brunner, D., Bzumle, M., Meier, M., Keiser, S., Stahelf, W., Kellerf, C., 1995. Emission factors from road traffic from a tunnel study (Gubrist tunnel, Switzerland). Part I: concept and first results. Sci. Total Environ. Environ. 169, 141–147.

Thorpe, A., Harrison, R.M., 2008. Sources and properties of non-exhaust particulate matter from road traffic: a review. Sci. Total Environ. https://doi.org/10.1016/j.scitotenv.2008.06.007.

Wedepohl, H.K., 1995. The composition of the continental crust. Geochim. Cosmochim. Acta 59, 1217–1232. https://doi.org/10.1016/0016-7037(95)00038-2.

Widziewicz-Rzońca, K., Tytła, M., 2020. First Systematic Review on PM-Bound Water: Exploring the Existing Knowledge Domain Using the CiteSpace Software, Scientometrics. Springer International Publishing. https://doi.org/10.1007/s11192-020-03547-w.

Zhou, R., Wang, S., Shi, C., Wang, W., Zhao, H., Liu, R., Chen, L., Zhou, B., 2014. Study on the traffic air pollution inside and outside a road tunnel in Shanghai, China. PLoS One 9, 1–9. https://doi.org/10.1371/journal.pone.0112195.